Intense turbulence observed above a mesospheric temperature inversion at equatorial latitude

G. A. Lehmacher,[1] C. L. Croskey,[2] J. D. Mitchell,[2] M. Friedrich,[3] F.-J. Lübken,[4] M. Rapp,[4] E. Kudeki,[5] and D. C. Fritts[6]

Received 9 August 2005; revised 21 September 2005; accepted 6 October 2005; published 28 April 2006.

[1] Results from a sounding rocket experiment launched on September 19, 2004 from Kwajalein Atoll, Marshall Islands are reported. A large modulation of the temperature profile in the upper mesosphere was observed with a local maximum at 92 km, 40 K warmer than 2 km below. The temperature gradient between 92 and 102 km was near-adiabatic, suggesting strong mixing. Turbulence was observed in the lower part of the mixed layer, as evidenced by neutral and plasma density fluctuations on both the upleg and downleg portions of the flight. The plasma density gradient was less steep in the mixed region. The turbulent energy dissipation rate was found to be 170 mW/kg. The thermal structure can be described as an upper mesospheric inversion layer, possibly caused by enhanced wave breaking or turbulent heat transport. **Citation:** Lehmacher, G. A., C. L. Croskey, J. D. Mitchell, M. Friedrich, F.-J. Lübken, M. Rapp, E. Kudeki, and D. C. Fritts (2006), Intense turbulence observed above a mesospheric temperature inversion at equatorial latitude, *Geophys. Res. Lett.*, *33*, L08808, doi:10.1029/2005GL024345.

1. Introduction

[2] The mesopause is usually well defined during summer at mid- and high latitudes exhibiting a very low temperature minimum near 89 km. However, during the rest of the year at those latitudes and all year long at low and equatorial latitudes, it is not as distinct and departs less from radiative equilibrium because the mean wave forcing is less dramatic. Mesospheric temperature inversions frequently occur at low and midlatitudes and induce large-scale modulations, often in the upper mesosphere above ~80 km [e.g., *Hauchecorne et al.*, 1987; *Meriwether and Gerrard*, 2004]. Such structures have been attributed to nonlinear wave interactions involving tides, since inversions often slowly descend with similar phase speeds. They persist over hours, may extend over hundreds of kilometers, and their occurrence varies in latitude and season. Model simulations of mesospheric inversion layers predict strong local and inhomogeneous heating and cooling due to advection, turbulent diffusion, and energy dissipation [*Liu et al.*, 2000; *Liu and Meriwether*, 2004]. However, the observation of subgrid dynamical scales, relevant for the generation of neutral turbulence, requires in situ measurements with instrumented rockets.

[3] This paper describes the observation of a large-scale temperature modulation in the mesopause region based on measurements performed during the NASA EQUIS II rocket campaign. We observed both small-scale neutral and plasma fluctuations to distinguish neutral turbulence from plasma instabilities [*Lehmacher et al.*, 1997]. The science target was the distribution and magnitude of turbulence in the mesosphere at a low-latitude site. We may expect some differences compared to mid- and high-latitude cases [e.g., *Lübken et al.*, 1993] due to the very different mean and large- and small-scale wave motions.

[4] The next section briefly explains the instrumentation and methods used to obtain temperatures, electron densities and turbulence spectra. We then present our results, a deep turbulence layer just above a temperature inversion, and associated stability and wind measurements. We also discuss our observations in comparison with other turbulence data and model results, and summarize our findings.

2. Instrumentation and Data Analysis

[5] The sounding rocket was launched on September 19, 2004 at 23:30 UT (11:30 LT) from Roi-Namur, Kwajalein Atoll, Marshall Islands (9°N, 168°E). The front of the payload was equipped with a nosetip probe (NTP) that operated on both the upleg and downleg portions of the flight to collect electrons and negative ions [*Smith*, 1969]. A radio wave propagation experiment used ground-based transmitters and rocket-borne receivers to determine *D* and *E* region electron densities from Faraday rotation and differential absorption [e.g., *Mechtly*, 1974]. The CONE (Combined Neutral and Electron) sensor, which is an open, spherical, hot-cathode ionization gauge with the outermost electrode biased for electron collection, was centrally mounted on the aft end of the payload [*Giebeler et al.*, 1993]. A pair of screened positive ion probes (PIP) on short booms and a pair of screened blunt probes complemented the aft end instrumentation [*Croskey et al.*, 2001]. The steerable ALTAIR 422-MHz UHF radar received electron incoherent backscatter between ~80 and 700 km. Compre-

[1]Department of Physics and Astronomy, Clemson University, Clemson, South Carolina, USA.
[2]Communications and Space Sciences Laboratory, Department of Electrical Engineering, Pennsylvania State University, University Park, Pennsylvania, USA.
[3]Institute for Communications Networks and Satellite Communication, Graz University of Technology, Graz, Austria.
[4]Leibniz-Institute for Atmospheric Physics, Kühlungsborn, Germany.
[5]Department of Electrical and Computer Engineering, University of Illinois, Urbana, Illinois, USA.
[6]Colorado Research Associates, Northwest Research Associates, Boulder, Colorado, USA.

0094-8276/06/2005GL024345$05.00

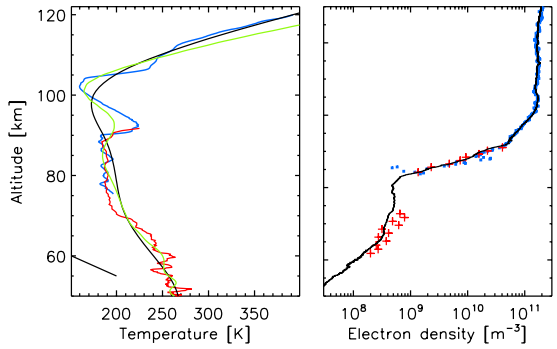

Figure 1. (left) Temperatures measured by ionization gauge CONE (blue) and falling sphere (red). For comparison we show MSIS temperatures (black) and SABER data (green) from two overpasses on September 16, ~14:20 LT. The slanted line near 60 km indicates the adiabatic lapse rate. (right) Absolute electron densities from ALTAIR radar (blue), Faraday rotation and differential absorption (red) and normalized nosetip probe data (black).

hensive presentations of the plasma density measurements will be given by *Friedrich et al.* [2006].

[6] The CONE ionization gauge measured a neutral density profile which has been corrected for the density increase caused by the supersonic flow in the rarefied atmosphere [*Rapp et al.*, 2001]. The temperature profile (Figure 1) is calculated by integrating the densities from 120 km down, assuming hydrostatic equilibrium and a start temperature taken from the extended MSIS model [*Hedin*, 1991]. Additional density, temperature and horizontal wind profiles below ~90 km come from three passive falling spheres [*Schmidlin*, 1991], which were launched from Kwajalein Island, ~80 km to the south, at 10:50, 12:01, and 14:00 LT. Absolute electron densities were obtained from the combination of rocket-borne Faraday rotation, incoherent scatter from the calibrated ALTAIR radar, and NTP measurements (Figure 1).

[7] Neutral and plasma density fluctuations are obtained from fast and sensitive, low-noise and high-gain, logarithmic electrometers. The DC channels are unfiltered, direct-current measurements, while for the AC channels the signal is further amplified and high-pass filtered to suppress the spin frequency at 5.5 Hz. For NTP and CONE the signals were converted to 24-bit serial data and sampled at 5000 Hz. For short data intervals the output is proportional to the logarithm of the density, and therefore a small change in the data is proportional to the relative density fluctuation $\Delta n/n$.

[8] The turbulent energy dissipation rate is determined from the fluctuation spectra as described by *Lübken* [1992]. The turbulence spectrum exhibits a transition from the inertial subrange with Kolmogorov's well-known $-5/3$ slope to the viscous subrange with a steeper slope, for example, -7, as suggested by *Heisenberg* [1948]. This break in the spectrum occurs at the inner scale l_0, which is proportional to the microscale η; in case of Heisenberg's model $l_0 = 9.9\eta$. The turbulent energy dissipation rate $\varepsilon = (9.9/l_0)^4\nu^3$ is calculated from the inner scale l_0 determined by a best fit of the fluctuation spectrum. The kinematic viscosity $\nu \sim 1/\rho$ is derived from our simultaneous density and temperature measurements.

[9] Between 92 and 96 km, large electron density fluctuations of ~10% are observed (Figure 2). The FFT spectrum for these data, together with the best fit of the model spectrum, is shown in the same figure below. The inner scale was found to be $l_0 = 80 \pm 10$ m, and the average energy dissipation rate $\varepsilon = 170 \pm 70$ mW/kg, corresponding to a turbulent dissipation heating rate of 15 K/d. Turbulent fluctuations of neutrals and electrons with similar power spectra were also observed on downleg in the same region [*Lehmacher et al.*, 2005].

3. Results

[10] The most striking feature is the large-scale temperature modulation between 90 and 105 km. Between 92 and 102 km the temperature gradient is nearly adiabatic, indicating either mixing of the temperature profile, large vertical advection, or both, extending over a deep layer. The atmosphere is very stable near 90 and 105 km.

[11] The electron density profile is typical for the daytime equatorial ionosphere with a distinct *E* region ledge between 85 and 90 km. Superimposed are distinct layers characterized by different electron density gradients. Above 92 km the gradient is markedly less steep, and in the same altitude range the nearly adiabatic temperature gradient is observed. Around 105 km, a region of decreasing electron densities is found.

[12] Neutral density fluctuations caused by vertical adiabatic motions are proportional to the square of the buoyancy frequency $N^2 = g\partial\ln\theta/\partial z = (g/T)(\partial T/\partial z + g/c_p) = g(1/H - 1/\gamma H_p)$. Ion and electron density fluctuations embedded in the motion are different (often larger) by a factor of $1/H_{i,e} - 1/(\gamma H_n)$ and opposite due to their opposite background gradient [*Thrane and Grandal*,

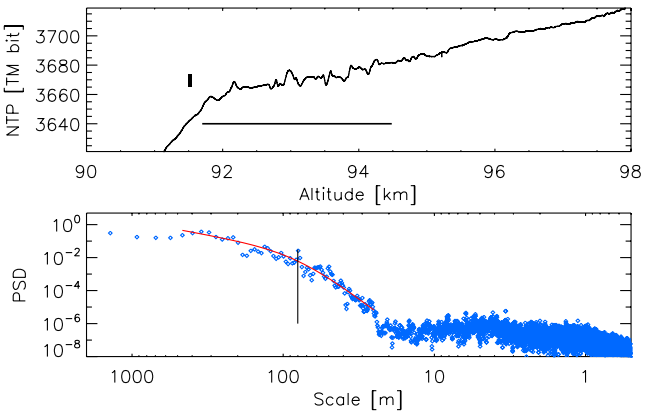

Figure 2. (top) Electron density fluctuations observed by the NTP on the upleg portion of the flight. The small vertical bar indicates a fluctuation of 10%. (bottom) Power spectrum of the fluctuations indicated by the horizontal line and smoothed with a 3-point running average. The red line is the best fit of a Heisenberg spectrum, and the vertical line shows the inner scale. Results are $l_0 = 80 \pm 10$ m, $\varepsilon = 170 \pm 70$ mW/kg. Payload speed was 850 m/s, and dynamic viscosity 9 m^2/s.

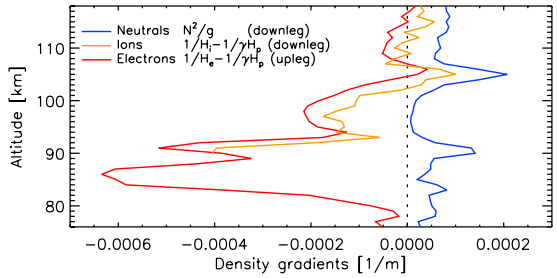

Figure 3. Density gradients relevant for the observation of vertical adiabatic motions in a stable atmosphere. Neutral fluctuations are proportional to N^2/g. Plasma density fluctuations embedded in the motion are different by a factor $1/H_{i,e} - 1/(\gamma H_n)$.

1981]. $H_i = -\partial \ln(n_i)/\partial z$ etc. are the scale heights, and $\gamma = c_p/c_v = 1.4$ for air. Figure 3 shows these scale factors determining the level of fluctuations. In the region between 93 and 102 km, $N^2$is close to zero, indicating very low static stability. The plasma density gradient is large in the ledge region, amplifying the turbulent fluctuations; a small positive neutral density excursion will cause a large negative plasma density change. The mixing by turbulence weakens the plasma density gradient near 92–94 km, as seen in the peaks in the profile. At 105–106 km the plasma density gradient changes, as indicated by the sign change and coinciding with a layer having a very stable temperature profile. Ion density gradients for the downleg portion of the flight have been derived from the measured ion current as a proxy for ion density above 88 km. It follows the same basic pattern, is shifted downward by about 1 km compared to the electron measurements on the upleg. Based on the trajectory, a northward and downward tilt of ~1/35 is observed, which might be caused by a low-frequency gravity wave motion.

[13] Falling sphere profiles of zonal and meridional wind are shown in Figure 4 together with estimates from the Global Scale Wave Model, a spectral model calculating the structure of diurnal and semidiurnal migrating and nonmigrating tides [*Hagan and Forbes*, 2002]. The close match in the meridional wind suggests that the major diurnal (1,1)-mode with a vertical wavelength of ~25 km showed a normal level of activity. Other evidence for tidal motion is derived from descending electron density valleys around 105 and 120 km as observed with ALTAIR (E. Kudeki et al., ALTAIR incoherent scatter observations of the equatorial daytime ionosphere, submitted to *Geophysical Research Letters,* 2005), the zonal wind profiles have a prominent easterly maximum at 80 km, which can be attributed to the fall equinox phase of the mesosphere semiannual oscillation [*Garcia et al.*, 1997] not contained in the model.

4. Discussion

[14] The observed temperature structure around 90 km may be labeled a mesospheric inversion layer [e.g., *Meriwether and Gerrard*, 2004]. Such layers are not uncommon, as shown in a recent survey based on SABER temperature profiles [*Picard et al.*, 2004] and indeed, the closest overpasses from SABER, three days earlier at 1420 LT, indicate a similar temperature structure (cf. Figure 1). *Picard et al.* find a clear semiannual modulation in the frequency of equatorial inversion layers around 90 km, with maxima around the equinoxes, which was the time of our launch.

[15] It was suggested by *Hauchecorne et al.* [1987] that strong gravity wave breaking may occur at inversion layers, since the wave saturation ratio, defined as quotient of the saturated and unsaturated temperature amplitude, increases as $N/|c - \bar{u}|^3$. *Hauchecorne et al*. argued that the induced turbulence causes strong downward heat transport and thus maintains the inversion layer. The theory of enhanced wave saturation was further developed by *VanZandt and Fritts* [1989], and a similar event has recently been observed during polar summer [*Fritts et al.*, 2004]. Furthermore, we observe a 10 km deep layer with an adiabatic temperature gradient above the inversion. This length scale was predicted as the dominant vertical wavelength.

[16] *Liu et al.* [2000] have generated inversion layers in a model including nonlinear wave interaction with tides. Their result for equinox conditions at the equator resembles very much the measurements described here. They found total heating rates of ~10 K/h maintaining the inversion, mostly associated with wave and turbulent heat transports in the lower part of the wave-breaking region. Large heating rates due to wave advection and turbulent transport were also obtained from a study in the lower mesosphere, while the largest dissipative heating of 1 K/h (280 mW/kg) occurred just above the inversion [*Liu and Meriwether*, 2004].

[17] The falling sphere meridional wind measurements (Figure 4) in comparison with the tidal model clearly illustrate the presence of the diurnal tide. While there are limitations inherent in the falling sphere data above 85 km, the observations show a tendency for the tidal wavelength to be shortened below 90 km and suggest large wind shears around the inversion layer. Furthermore, the strong westward flow around 80 km caused by the superposition of tides and the mesospheric semiannual oscillation may have had an impact on the propagation of gravity waves reaching the upper mesosphere.

[18] The observed energy dissipation rate of 170 mW/kg is large compared to 10–20 mW/kg obtained in polar winter and equinox [*Lübken*, 1997]. Values of 10–100 mW/kg

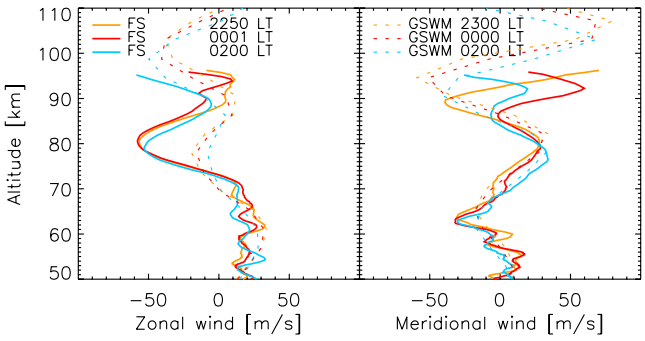

Figure 4. Horizontal winds measured by three falling spheres launched from Kwajalein Island and compared to GSWM data.

have been reported from measurements over Brazil [*Lehmacher et al.*, 1997]. Our rates are also compatible with results from recent measurements of the diffusion of luminescent vapor trails at White Sands, NM [*Bishop et al.*, 2004]. They observed values of 50–140 mW/kg between 87 and 93 km in a deep, near-adiabatic layer. Our results are strong evidence that turbulence, both via turbulent heating and downward heat transport, is a factor in maintaining inversion layers. The weaker turbulence at high latitudes [*Lübken*, 1997] may be related to the low-occurrence frequency of upper inversion layers [*Picard et al.*, 2004]. However, it should be noted that our observations were made during the maximum of the observed diurnal and seasonal variability pattern.

[19] A second very stable layer is present near 103 km, followed by a less stable region in the lower thermosphere, which is associated with a layer of decreasing electron density in the lower *E* region. A temperature profile from an instrumented falling sphere launched from Kwajalein Atoll on May 18, 1977, 1342 LT exhibits a similar modulation with the absolute minimum at 102 km and a steep gradient around 107 km [*Philbrick et al.*, 1978]. *Picard et al.* [2004] reported regular observations of large CO_2 infrared radiances in the equatorial lower thermosphere around 105 km that could be associated with a temperature signature. In the same region, very large horizontal winds and wind shears are often present in chemical trail observations [*Larsen*, 2002] suggesting instabilities and large diffusion rates.

5. Summary and Conclusions

[20] We have presented the first simultaneous observations of turbulent density fluctuations associated with a mesospheric inversion near 90 km at an equatorial latitude. Turbulence was best observed in the electron densities, since the layer occurred at the *E* region ledge, which enhances plasma over neutral fluctuations. The energy dissipation rate was 170 mW/kg, which is large compared to similar measurements at winter high latitudes. The observations suggest that enhanced wave dissipation occurs at and above the inversion, and wave and turbulent transports and turbulent heating are the significant sources that create and maintain such a structure. The observation took place near fall equinox, when inversion layers are frequent. Meridional winds show that the diurnal tide participates in the wave action.

[21] While we have concentrated on turbulence above 90 km, we also see evidence for steep sawtoothlike temperature changes between 60 and 90 km with adiabatic lapse rates. At the same time the *D* region plasma structure is modulated, with gradient changes at similar vertical scales, including regions of constant plasma density. Inertia-gravity waves with 2–3 km vertical wavelength are important at low latitudes. However, turbulence in the middle and lower mesosphere is expected to be much smaller (1–10 mW/kg). Our fluctuation data will require further analysis, but we anticipate that our results will be relevant to mesospheric turbulent layers observed with VHF radars.

[22] **Acknowledgments.** The project was supported by NASA grants NAG 5-5385, 5-5369, 5-2069, 5-2060, and Austrian Research Fund grant 15985. The CONE sensors were manufactured by H.-J. Heckl (IAP). Instrumentation and field support were provided by M. Wharton (Penn State University). Falling sphere data were processed by K. McGrath (3D Research), and F. Schmidlin and A. Beebe (WFF). We thank D. Sponseller and the radar staff for operating the ALTAIR system. We especially thank M. Larsen and the teams from WFF and USAKA/RTS for organizing the EQUIS II campaign. M. Hagan and C. Mertens provided GSWM and SABER data for wind and temperature comparisons.

References

Bishop, R. L., et al. (2004), TOMEX: Mesospheric and lower thermospheric diffusivities and instability layers, *J. Geophys. Res.*, *109*, D02S03, doi:10.1029/2002JD003079.

Croskey, C. L., J. D. Mitchell, M. Friedrich, K. M. Torkar, U.-P. Hoppe, and R. A. Goldberg (2001), Electrical structure of PMSE and NLC regions during the DROPPS program, *Geophys. Res. Lett.*, *28*, 1427–1430.

Friedrich, M., et al. (2006), Rocket and incoherent scatter radar common-volume electron measurements of the equatorial lower ionosphere, *Geophys. Res. Lett.*, *33*, L08807, doi:10.1029/2005GL024622.

Fritts, D. C., B. P. Williams, C. Y. She, J. D. Vance, M. Rapp, F.-J. Lübken, A. Müllemann, F. J. Schmidlin, and R. A. Goldberg (2004), Observations of extreme temperature and wind gradients near the summer mesopause during the MaCWAVE/MIDAS rocket campaign, *Geophys. Res. Lett.*, *31*, L24S06, doi:10.1029/2003GL019389.

Garcia, R. R., T. J. Dunkerton, R. S. Lieberman, and R. A. Vincent (1997), Climatology of the semiannual oscillation of the tropical middle atmosphere, *J. Geophys. Res.*, *102*, 26,019–26,032.

Giebeler, J., et al. (1993), CONE—A new sensor for in situ observations of neutral and plasma density fluctuations, *Eur. Space Agency Spec. Publ., ESA-SP 355*, 311–318.

Hagan, M. E., and J. M. Forbes (2002), Migrating and nonmigrating diurnal tides in the middle and upper atmosphere excited by tropospheric latent heat release, *J. Geophys. Res.*, *107*(D24), 4754, doi:10.1029/2001JD001236.

Hauchecorne, A., M. L. Chanin, and R. Wilson (1987), Mesospheric temperature inversion and gravity wave dynamics, *Geophys. Res. Lett.*, *14*, 933–936.

Hedin, A. E. (1991), Extension of the MSIS thermosphere model into the middle and lower atmosphere, *J. Geopys. Res.*, *96*, 1159–1172.

Heisenberg, W. (1948), Zur statistischen Theorie der Turbulenz, *Z. Phys.*, *124*, 628–657.

Larsen, M. F. (2002), Winds and shears in the mesosphere and lower thermosphere: Results from four decades of chemical release wind measurements, *J. Geophys. Res.*, *107*(A8), 1215, doi:10.1029/2001JA000218.

Lehmacher, G., R. A. Goldberg, F. J. Schmidlin, C. L. Croskey, J. D. Mitchell, and W. E. Swartz (1997), Electron density fluctuations in the equatorial mesosphere: Neutral turbulence or plasma fluctuations?, *Geophys. Res. Lett.*, *24*, 1715–1718.

Lehmacher, G., et al. (2005), Layers in the equatorial mesosphere: Results from rocket and radar measurements during EQUIS II, *Eur. Space Agency Spec. Publ.*, *ESA-SP 590*, 167–172.

Liu, H., and J. W. Meriwether (2004), Analysis of a temperature inversion event in the lower mesosphere, *J. Geophys. Res.*, *109*, D02S07, doi:10.1029/2002JD003026.

Liu, H.-L., M. Hagan, and R. Roble (2000), Local mean state changes due to gravity wave breaking modulated by the diurnal tide, *J. Geophys. Res.*, *105*, 12,381–12,396.

Lübken, F.-J. (1992), On the extraction of turbulent parameters from atmospheric density measurements, *J. Geophys. Res.*, *97*, 20,385–20,395.

Lübken, F.-J. (1997), Seasonal variation of turbulent energy dissipation rates at high latitudes as determined by in situ measurements of neutral density fluctuations, *J. Geophys. Res.*, *102*, 13,441–13,456.

Lübken, F.-J., W. Hillert, G. Lehmacher, and U. von Zahn (1993), Experiments revealing small impact of turbulence on the energy budget of the mesosphere and thermosphere, *J. Geophys. Res.*, *98*, 20,369–20,384.

Mechtly, E. A. (1974), Accuracy of rocket measurements of lower ionosphere electron density concentrations, *Radio Sci.*, *9*, 373–378.

Meriwether, J. W., and A. J. Gerrard (2004), Mesosphere inversion layers and stratosphere temperature enhancements, *Rev. Geophys.*, *42*, RG3003, doi:10.1029/2003RG000133.

Philbrick, C. R., et al. (1978), Measurements of atmospheric density at Kwajalein Atoll, 18 May 1977, *AFGL-TR-78–0058*, Air Force Geophys. Lab., Bedford, Mass.

Picard, R. H., et al. (2004), Tidal and layer structure in the mesosphere and lower thermosphere from TIMED/SABER CO_2 15-μm emission, *Proc. SPIE Int. Soc. Opt. Eng.*, *5571*, 182–192, doi:10.1117/12.568060.

Rapp, M., et al. (2001), Absolute density measurements in the middle atmosphere, *Ann. Geophys.*, *19*, 571–580.

Schmidlin, F. J. (1991), The inflatable sphere: A technique for the accurate measurement of middle atmosphere temperatures, *J. Geophys. Res.*, *96*, 22,673–22,682.

Smith, L. (1969), Langmuir probes in the ionosphere, in *Small Rocket Instrumentation Techniques*, Elsevier, New York.

Thrane, E. V., and B. Grandal (1981), Observations of fine scale structure in the mesosphere and lower thermosphere, *J. Atmos. Terr. Phys.*, *43*, 179–189.

VanZandt, T. E., and D. C. Fritts (1989), A theory of enhanced saturation of the gravity wave spectrum due to increases in atmospheric stability, *Pure Appl. Geophys.*, *130*, 399–420.

C. L. Croskey and J. D. Mitchell, Communications and Space Sciences Laboratory, Department of Electrical Engineering, Pennsylvania State University, University Park, PA 29631, USA.

M. Friedrich, Institute for Communications Networks and Satellite Communication, Graz University of Technology, Inffeldgasse 12, A-8010 Graz, Austria.

D. C. Fritts, Colorado Research Associates, Northwest Research Associates, 3380 Mitchell Lane, Boulder, CO 80301, USA.

E. Kudeki, Department of Electrical and Computer Engineering, University of Illinois, Urbana, IL 61801, USA.

G. A. Lehmacher, Department of Physics and Astronomy, 105 Kinard Lab, Clemson University, Clemson, SC 29634, USA. (glehmac@clemson.edu)

F.-J. Lübken and M. Rapp, Leibniz-Institute for Atmospheric Physics, Schloss-Str. 6, D-18225 Kühlungsborn, Germany.